VAMPIRE® fundus image analysis algorithms

Cirla, Alessandro; Drigo, Michele; Ballerini, Lucia; Trucco, Emanuele; Barsotti, Giovanni

Published in:
Veterinary Ophthalmology

DOI:
10.1111/vop.12657

Publication date:
2019

Document Version
Peer reviewed version

VAMPIRE® fundus image analysis algorithms: validation and diagnostic relevance in hypertensive cats

Alessandro Cirla,*·†DVM, PhD Michele Drigo,‡ DVM, PhD Lucia Ballerini,§ PhD Emanuele Trucco§ PhD and Giovanni Barsotti† DVM, PhD

*Department of Ophthalmology, San Marco Veterinary Clinic and Laboratory – Veggiano, PD, Italy; †Department of Veterinary Science, University of Pisa – S. Piero a Grado, PI, Italy; ‡Department of Animal Medicine, Production and Health, University of Padova – Legnaro, PD, Italy and § School of Computing, University of Dundee – Dundee, Scotland

The authors declare no financial interests with companies that manufacture products that are the subject of the present research or with companies that manufacture competing products.

Corresponding author: Alessandro Cirla

San Marco Veterinary Clinic and Laboratory

Via dell'Industria 3, 35030 – Veggiano, PD, Italy

Tel.: +39-049-856-1098

Fax: +39-049-796-9254

e-mail: alessandro.cirla@sanmarcovet.it

Abstract

Objectives: To validate a retinal imaging software named VAMPIRE® (Vascular Assay and Measurement Platform for Images of the Retina) in feline patients and test the clinical utility in hypertensive cats.

Animals studied: One hundred and five healthy cats were enrolled. They represented the normal dataset used in the validation (group 1). Forty-three hypertensive cats with no noticeable retinal abnormalities were enrolled for the clinical validity of the software (group 2).

Procedures: Eleven points (4 veins, 4 arteries and 3 arterial bifurcations) were measured for each digital image. Repeatability and reproducibility of measurements were assessed using two independent operators. Data were statistically analyzed by the Mann-Whiney and Tukey box-plot. Significance was considered when $P<0.05$.

Results: Two hundred and ten retinal images were analyzed for a total of 2310 measurements. Total mean was 9.1 and 6.1 pixels for veins and arteries, respectively. First, second and third arteriolar bifurcations angles were 73.6°, 76.9° and 85.4°, respectively. A comparison between groups 1 and 2 showed a statistically significant reduction in arteriolar diameter (mean 3.3 pixels) and branch angle (55°, 47.8° and 59.9°) associated with increasing vein diameter (mean 24.15 pixels). Conclusions*:* Current image analysis techniques used in human medicine were investigated in terms of extending their use to veterinary medicine. The VAMPIRE® algorithm proved useful for an objective diagnosis of retinal vasculature changes secondary to systemic hypertension in cats, and could be an additional **diagnostic** test for feline systemic hypertension.

Key Words: cat, fundus, image analysis algorithms, software validation, retinal photography, systemic hypertension

INTRODUCTION

Arterial systemic hypertension is a clinical condition in which the blood pressure in the arteries is higher than its physiological values. Arterial hypertension is often correlated to systemic pathologies and is increasingly considered a cause of morbidity and, in some cases, death, both in humans and veterinary patients (1, 2, 3, 4, 5).

The eye, like the kidneys, heart and encephalon, is one of the target organs of the persistent hypertensive state. (6, 7, 8, 9, 10, 11, 12, 13, 14) At the ocular and particularly the retinal level, damage due to hypertension often causes sudden blindness although, at least in humans, this is increasingly less frequent thanks to early diagnosis of the disease. (12, 13, 14, 15)

Systemic hypertension is commonly found in cats, and often causes secondary ocular lesions. (4, 6, 8, 13, 16, 17, 18) Characteristic ocular lesions are the result of the rupture of the retinal endothelial barrier, and ischemia of the vascularisation of the choroid. The most common lesions associated with hypertension include intra/subretinal oedema, retinal hemorrhages and retinal detachment. (1, 2, 3, 4, 6, 8, 11, 12, 13, 14, 16) The literature on the ocular manifestations of feline hypertension is based on information and data derived from clinical practice. (1, 3, 4, 8, 10, 17) Inevitably the disease is already in the advanced stages at the time of clinical presentation and diagnosis, and blindness is the most evident clinical sign.

The retina is an excellent window for studying microcirculation both in physiological and pathological conditions. Retinal vessels, which can easily be seen using non-invasive methods, also share similar physiological characteristics to encephalic and cardiac microcirculation. **(4, 6, 8, 12,16, 17)** Therefore, recognizing the early signs of hypertensive retinopathy is key not only in order to preserve the anatomical and functional integrity of the eye but also to shed light on a complex system which affects other organs and vital systems.

Analysis of the retinal vascular structures provides a unique opportunity in that these are the only components of the entire circulatory system that can be observed in a non-invasive manner. The diagnosis of hypertensive retinopathy is qualitative and takes place via direct analysis of the fundus

using ophthalmoscopes (direct and indirect). However, this diagnosis is subjective and consequently lacking in reliability. This kind of analysis is clinical, whereas a better solution is automatic or semiautomatic retinal image analysis. A fundus camera facilitates the collection of retinal images which can then be analysed objectively. Photographing the fundus makes it possible to obtain high resolution images of large retinal areas, including the microcirculation, and provides objective documentation of the major retinal vessels and their bifurcations. (19) Defining an ideal instrument (objective and non-invasive) for assessing retinal vessels in human medicine has long been linked to using computer aided algorithms for measuring the properties of retinal vessels. (19, 20, 21, 22, 23, 24, 25, 26, 27, 28, 29) On the other hand, no such publications are available in recent veterinary literature where the analysis of the retinal vasculature is typically still correlated to the subjectivity of the observer.

The aim of this study was to verify whether Vascular Assessment and Measurement Platform for Images of the Retina software (VAMPIRE®) can be validated in veterinary medicine, and can help in the early diagnosis of retinal vasculature changes due to systemic hypertension in cats.

MATERIALS AND METHODS

This research was approved by the Agency for Animal Welfare of Pisa University (22/16) and developed with the coordination of the Department of Veterinary Science (Pisa University), in cooperation with the School of Computing (Dundee University, Scotland) and the Department of Animal Medicine, Productions and Health (Padua University). All the patients enrolled were examined in the same clinic (San Marco Veterinary Clinic and Laboratory, Padua).

Animal enrolment

One hundred and five clinically healthy cats (group 1) were enrolled for the validation of VAMPIRE® during a one-year period **and** represented the normality dataset used for the validation. **Out of 159** hypertensive cats **that** underwent a complete ophthalmic examination**, 43** cats with no noticeable retinal abnormalities but clinically diagnosed with hypertension **(**group 2) were enrolled

for the assessment of the software potential clinical applications. **Overall 116** cats were excluded from the study because of hyphema (12/116), retinal hemorrhages (48/116), bullous (24/116) and complete (32/116) retinal detachment.

Clinical examination group 1

All cats underwent a physical examination which included measurements of body temperature, pulse, respiratory rate, hydration status, thoracic auscultation, abdominal palpation and palpation of the ventral neck to detect enlarged thyroid gland. Systemic **blood** pressure was assessed using a high-definition oscillometry (petMAP®, Ramsey Medical Inc, Tampa, Florida, United States). Each cat was allowed 15 minutes to acclimatize to the clinic environment with the owner present, in a setting with no stimuli, and systemic pressure was measured before performing any clinical procedure. The appropriately sized cuff (size 3.0 cm) was applied at the base of the tail with the cat in a sternal-recumbent position. The same operator carried out three sequential measurements at one-minute intervals. Blood pressure values (systolic and diastolic) were calculated as the mathematical mean of the three measurements. The measurements taken in agitated or moving cats were eliminated, as were those in which the heart rate measured with the instrument differed from the heart rate measured manually by more than 50 beats per minute.

Anamnestic and clinical information were analysed in order to exclude current or prior systemic diseases.

Clinical examination group 2

All the cats underwent a clinical examination using the procedure described above for group 1. Cats with a systolic pressure equal to or higher than 160 mmHg and diastolic pressure equal to or higher than 100 mmHg were considered hypertensive.

All the cats underwent diagnostic procedures including laboratory diagnostics to help reach a diagnosis. All the blood samples were taken from the jugular vein. The urine samples were taken via cystocentesis. All tests were carried out at the same clinic (San Marco Veterinary Clinic and Laboratory) and always included:

1. **Complete** blood count **(CBC)**;
2. complete biochemical profile;
3. coagulation profile;
4. serum electrophoresis;
5. thyroid function tests (TSH, TT4 fT4);
6. urine test (urinary dipstick, specific gravity on refractometer, osmolality, urinary protein to urinary creatine ratio, microscopic sediment).

To formulate a reliable etiological diagnosis, each cat underwent a cardiology consultation and, where necessary, imaging diagnostic procedures such as thoracic radiographs, electrocardiography, abdominal and thyroid ultrasound were performed.

Ophthalmic examination and photographic documentation of the fundus (groups 1 and 2)

Each cat underwent an ophthalmic examination, carried out in a dark room where there were no stimuli, with minimal physical restriction. Complete ophthalmic examination always included neurophthalmic examination (palpebral reflex, assessment of menace response, pupillary light and dazzle reflexes), slit-lamp biomicroscopy (SL-15 portable Slit lamp, Kowa Company, Tokyo, Japan) and indirect ophthalmoscopy (Heine Omega 500 Unplugged and Heine 30D lens; Heine Instruments, Herrsching, Germany). Retention of corneal sodium fluorescein dye (HS Haag-Streit International fluorescein, Switzerland) and intraocular pressure estimation (TonoPen Vet, Reichert Inc, Depew, NY, USA) were performed.

For the photographic documentation of the fundus of the cats included in the study, a digital fundus camera for veterinary use (Clearview, Optibrand LLc, Ft Collins, Columbia, United States) was employed.

To prevent alteration of the anatomic characteristics of the retinal vasculature, both eyes were always examined without pharmacological dilation. (29)

A standard image shot centered on the optic disc was also defined, to allow the correct visualisation of the retinal vascular tree (arteries, veins and arteriolar bifurcations). The images obtained using

this technique needed to be free from defects caused by movement. The deliberate absence of all identifying details prevented observers from recognising the images and, therefore, guaranteed a more objective judgement.

Imagine analysing methods

The program used for this project is semi-automatic, modified and adapted for measuring the feline fundus by the developers. The software algorithms are, therefore, able to calculate both vascular and arterial diameters and to measure the angles of the arteriolar bifurcations (Fig. 1).

With the VAMPIRE® platform, the image processing system consists of I) digitalising the retina and II) measuring it.

Digitalisation of the retina

Digitalising the retina entails:

1. Applying a monochrome filter to enhance the contrast and definition of the vascular tree;
2. Automatically defining the four standard measurement areas (SMA) identified with the letters A, B, C and D. Guidelines (GL) for measuring the vessels were automatically outlined within each of these areas (Figure 2.a);
3. Manual cataloguing the vessels as arterial and venous (three arteries and three veins) for the subsequent analysis of their diameters;
4. Selecting measuring points of the vessels for each SMA, defined as localised at the intersection between the GL and the vessel itself (Figure 2.b);
5. Identifying and selecting for the subsequent measurement the first, second and third arteriolar bifurcations (Figure 2.c).

Measurements

Information on the vascular diameters and the inner angle (α) of the first, second and third arteriolar bifurcations was obtained as follows:

1. For each vascular measurement point previously identified, the margins of the vessel were selected manually (Figure 3.a,b,c). The vascular diameter was calculated automatically;

2. For each arteriolar branch measurement point previously identified (mother vessel), the anatomical landmarks (daughter vessels) were selected manually for the subsequent automatic calculation of the inner angle α (Figure 3.d,e,f).

Assessment of intra- and inter-operator variability

In order to validate the use of VAMPIRE® (semiautomatic) in terms of repeatability and reproducibility, 35 healthy cats randomly selected from the 105 healthy cats were evaluated in relation to the following parameters: vein and artery for every SMA, first, second and third arteriolar bifurcations angle. Two observers (experiments) were used and three repetitions (tests) were made of the same measurement. Research Randomizer (www.randomizer.org) was used to randomly organise both the selection and the order of the images to analyse. It seems unlikely that the images were memorized by the operators due to the long interval between the different measuring sessions (three weeks) and the large number of vessels identified. **Repeatability and reproducibility were assessed in relation to their individual and combined effects on the overall variability of the measurements taken.**

Assessment of the software potential clinical application

To assess the software potential clinical application the measurements were compared by analysing the photographic images **from group 2 (hypertensive animals) and a subset from** group 1 (healthy cats). **The same parameters considered in the validation of VAMPIRE® were used to compare the group of 105 healthy cats and the group of 43 clinically hypertensive cats without evident abnormalities of the fundus. For the comparison of healthy and hypertensive cats the** measurements were taken on the right eye only.

Statistical analysis

After testing the normality of the data, the non-parametric Mann-Whitney test was used to compare the distribution of the values between healthy and hypertensive cats. Tukey box plot graphs were produced for the graphic visualisation of these distributions.

The level of statistical importance was set for values of $P<0.05$.

RESULTS

The cats belonging to group 1 (clinically healthy cats) represented the normality dataset of the retinal measurements taken. One hundred and five cats of the same breed (domestic short hair) were used: 55 males and 50 females with a mean **and median** of 55 months (minimum 48, maximum 78). A total of 210 retinal images **(right and left eyes)** were analysed. Eleven points (four veins, four arteries and three arterial bifurcations) were recognised and measured for each image, totalling 2310 measurements. **No statistical difference was found for each of the comparison assessed. Table 1 summarised the values of the measurements taken only on the right eye.and represent the reference parameters for cats.**

Group 2 was constituted by 43 hypertensive cats **(24 males and 20 females) that** met the criteria for inclusion in the study. Mean **and median** age was 138 months (minimum 120, maximum 185). Twenty-five cats were affected by chronic renal failure, 16 cats were affected by hyperthyroidism, and 2 cats presented both these diseases.

Intra- and inter-operator variability (repeatability and reproducibility)

Repeatability (r) and reproducibility (R) were blind tested by two independent operators who performed three series of measurements in a set consisting of 35 images at intervals of three weeks **(Figure 4)**. As no statistical difference was found between the measurements of the images of the right eye (OD) and the left eye (OS), both observers assessed OD only. Each observer performed a total of 1155 measurements **(i.e. 35 images multiplied by 11 points of evaluation).**

Lastly, the **coefficient of variation (CV)** was calculated, in terms of R and r, for every measurement area (Table **2**).

Comparison between the measurements taken in the two groups (healthy-hypertensive animals)

To assess the potential clinical applications of VAMPIRE®, 43 retinal images belonging to group 1 and group 2 were analysed. In hypertensive cats the statistical processing proved the existence of a statistically significant reduction ($P<0.001$) in arterial vascular diameter (group 1 mean 6.1 +/- 0.8; group 2 mean 3.3 +/- 1.4) and arteriolar branch angles (first arteriolar branch angle: group 1 mean

73.3° +/- 19°; group 2 mean 54.7° +/- 20.5°. Second arteriolar branch angle: group 1 mean 77.1° +/- 17.1°; group 2 mean 54.7° +/- 20.5°. Third arteriolar branch angle: group 1 mean 83.9° +/-15.2°; group 2 mean 59.9° +/- 24.7°) associated with an increase in vein diameter (group 1 9.1 +/- 1; group 2 16.1 +/- 4) as shown in Figure 5.

DISCUSSION

The results of the present study provide a validation of the semi-automatic software VAMPIRE® in cats. Our results cannot be compared with the current veterinary literature as no studies have been published in this field. In contrast, in human medicine some softwares for retinal imaging analysis has been validated, and some publications demonstrate their utility in the early diagnosis of retinal vasculature changes during systemic hypertension. (7,19, 20, 21, 23)

Our results showed that VAMPIRE® is consistent when giving interpretations. The results showed an optimum R for vein measurements (Mean **CV**: 1.1%) and a very good R for artery measurements (Mean **CV**: 3.1%) and bifurcation angles (Mean **CV**: 3.4%). In these last two groups, the Mean Variation Coefficient was higher in the standard measuring area (SMA) B for arterioles (Mean **CV**: 5%) and in the assessment of third arteriolar bifurcations (Mean **CV**: 9.3%). In fact, in SMA B, there is a higher overlapping of arteries and veins which could generate possible errors in clearly distinguishing and precisely identifying the arterial walls. The third arteriolar bifurcation angle (Mean **CV**: 9.3%) in the digital image was the least clear and most peripheral one, **prone** to more errors in interpretation.

Repeatability absorbs most of the total variability in measurements. Nevertheless, R shows that these measurements tend to comprise the same centre of measurement. “Poor” r must be considered in the light of the type of measurements taken, i.e. the possible discrepancy between these measurements and the possible sphere of variation, which is very slight. In the comparison between the two group measurements (clinically healthy and hypertensive cats), in the hypertensive cats there was a statistically significant reduction in the arteriolar diameter (mean total: 3.5 pixels) and

branch angles (55°, 47.8° and 24.7°), associated with an increase in the vein diameter (mean total: 24.15 pixels).

Microvascular dysfunction has been suggested to be a pathogenic factor for the development of systemic hypertension (5, 6). In human medicine retinal vascular calibre can be assessed non-invasively from retinal photographs and computer-assisted approaches (20, 21, 22, 25, 27, 28), while there is currently no data on the application of retinal imaging analysis software in veterinary medicine.

There are intrinsic limitations to the method analysed: the measurements, although taken in standardised anatomical landmarks, refer to very small anatomical structures; and errors in the procedure are possible. Consequently, the operator is a variable. The results of our analysis were based on a single-occasion retinal measurements, and lacks information on serial measurements. VAMPIRE® is semi-automatic, thus the measurements have to be taken manually. To date, also in human medicine most publications (20, 21, 27) on assessing the change in vascular changes (vascular calibre and bifurcation angles) in fundus images still rely on a semi-automatic tool. Huang *et al.* proposed an automatic quantitative width measurement for retinal blood vessels, validating the technique by comparing the results with VAMPIRE®. (28)

Based on the observations from this study, the development of future automated algorithms for medical veterinary imaging essentially entails collecting a larger dataset including both normal and abnormal cases. An automatic retinal vessel measurement technique will enable fully quantitative retinal vessel analyses in large-scale screening programs.

CONCLUSIONS

The image processing of color fundus images could potentially play a role in the diagnosis of hypertensive retinopathy in cats. The findings of the retina image analysis offer a new method for the early diagnosis of hypertension and objectively reflect the complex, but only partially

understood, physiopathological mechanisms at the base of the initial stages of this syndrome, both in cats and humans. The VAMPIRE® algorithm used to measure vascular diameters and angles of the arteriolar bifurcations contributes to the objective diagnosis of early damage to the ocular fundus as a result of systemic hypertension. It also facilitates an additional investigation into the effect of microvascularisation on the physiopathology of this complex syndrome.

REFERENCES

1. Bijsmans ES, Jepson RE, Chang YM *et al.* Changes in systolic blood pressure over time in healthy cats and cats with chronic kidney disease. *Journal of Veterinary Internal Medicine* 2015; 29:855-861.
2. Chetboul V, Lefebvre HP, Pinhas C *et al.* Spontaneous feline hypertension: clinical and echocardiographic abnormalities, and survival rate. *Journal of Veterinary Internal Medicine* 2003; 17:89-95.
3. Kobayashi DL, Peterson ME, Graves TK *et al*. Hypertension in cats with chronic renal failure or hyperthyroidism. *Journal of Veterinary Internal Medicine* 1990; 4:58-62.
4. Maggio F, De Francesco TC, Atkins CE *et al*. Ocular lesions associated with systemic hypertension in cats: 69 cases (1985-1998). *Journal of the American Veterinary Medicine Association* 2000; 217:695-702.
5. Oparil S. Zaman MA, Calhourn DA. Pathogenesis of hypertension. *Annals of Internal Medicine* 2003; 139:761-776.
6. Attariwale R, Giebs CP, Glucksberg MR. The influence of elevated intraocular pressure on vascular pressures in the cat retina. *Investigative Ophthalmology and Visual Science* 1994; 35:1019-1025.
7. Chew SK, Xie J, Wang JJ. Retinal arteriolar diameter and the prevalence and incidence of hypertension: a systemic review and meta-analysis of their association. *Current Hypertension Reports* 2012; 14:144-151.
8. Crispin SM, Mould JR. Systemic hypertensive disease and feline fundus. *Veterinay Ophthalmology* 2001; 4(2):31-140.
9. De Venecia G, Jampol LM. The eye in accelerated hypertension. II. Localized serous detachement of the retina in patients. *Archives of Ophthalmology* 1984;102(1):68-73.

10. Henik R, Snyder P, Volk L. Treatment of systemic hypertension in cats with amlodipine besylate. *Journal of the American Animal Hospital Association* 1997; 33:226-234.

11. Henik RA. Diagnosis and treatment of feline systemic hypertension. *Compendium on Continuing Educationfor the Practising Veterinarian* 1997; 19:163-179.

12. Morgan GE, Mikhail MS, Murray MJ. Systemic hypertension in four cats: ocular and medical findings. *Journal of the American Animal Hospital Association* 1986; 22:615-621.

13. Sansom J, Barnett KC, Dunn KA*et al.* Ocular disease associated with hypertension in 16 cats. *Journal of Small Animal Practice* 1994; 35:604-611.

14. Sansom J, Bodey A. Ocular sign in four dogs with hypertension. *Veterinary Record* 1997; 140:593-598.

15. Connell JM, Davies E. The new biology of aldosterone. *Journal of Endocrinology* 2005; 186:1-20.

16. Brown S, Atkins C, Bagley R *et al*. Guidelines for the identification, evaluation, and management of systemic hypertension in dogs and cats. *Journal of Veterinary Internal Medicine* 2007; 21-542-558.

17. Carter JM, Irving AC, Bridges JP*et al*. The prevalence of ocular lesions associated with hypertension in a population of geriatric cats in Auckland, New Zealand. *New Zealand Veterinary Journal* 2014; 62:21-29.

18. Anderson DH, Guerin CJ, Erikson PA *et al*. Morphological recovery in the reattached retina. *Investigative Ophthalmology and Visual Science*1986; 27:168-183.

19. Hubbard LD, Brothers RJ, King WN *et al*. Methods for evaluation of retinal microvascular abnormalities associated with hypertension/sclerosis in the Atherosclerosis Risk in Communities Study. *Ophthalmology* 1999; 106:2269-2280.

20. Abtamoff MD, Garvin MK, Sonka M. Retinal imaging and image analysis. *IEEE Review in Biomedical Engeneering* 2010; 3:169-208.

21. Abtamoff MD, Garvin MK, Sonka M. Retinal imaging and image analysis. *IEEE Review in Biomedical Engeneering* 2010; 3:169-208.

22. Bartling H, Wanger P, Martin L. Measurement of optic disc parameters on digital fundus photographs: algorithm development and evaluation. *Acta Ophthalmologica* 2008; 86:837-841

23. Ikram MK, De Jong FJ, Vingerling JR *et al*. Are retinal arteriolar or venular diametes associated with markers for cardiovascular disorders? The Rotterdam Study. *Investigative Ophthalmology and Visual Science* 2004; 45:2129-2134.

24. Ikram MK, Janssen JA, Roos AM *et al*. Retinal vessel diameters and risk of impaired fasting glucose or diabetes: the Rotterdam Study. *Diabetes* 2006; 55:506-510.

25. Knudston MD, Klein BE, Klein R *et al*. Variation associated with measurement of retinal vessel diameters at different points in the puls cycle. *British Journal of Ophthalmology* 2004; 88:57-61.

26. Mansour AM. Measuring fundus landmarks. *Investigative Ophthalmology and Visual Science* 1990; 31:41-42.

27. Trucco E, Ruggieri A, Karnowski T *et al*. Validating retinal fundus image analysis algorithms: issues and proposal. *Investigative Ophthalmology and Visual Science* 2013; 54:3546-3559.

28. Hunag F. Dashtbozorg B, Ka Shing Yeung A *et al.* A comparative study towards the establishment of an automatic retinal vessel width measurement technique. In: Cardoso M. et al. (eds) Fetal, Infant and Ophthalmic Medical Image Analysis. OMIA 2017, FIFI 2017. Lecture Notes in Computer Science, vol 10554. Springer, Cham

29. Harazny JM, Scmieder RE, Welzenbach J *et al*. Local application of tropicamide 0.5% reduces retinal capillary blood flow. *Blood Pressure* 2013; 22(6):371-376.

TABLES

Table 1 – Vascular reference parameters in normal feline fundus (measurements from OD expressed in px)

	Mean	Standard Deviation	Median	Min	Max	Percentile 25	Percentile 75
Vein A	9.0	0.6	8.9	7.7	11.8	8.6	9.1
Vein B	9.1	1.0	9.0	6.9	14.2	8.5	9.4
Vein C	9.1	0.8	9.2	7.1	11.8	8.5	9.4
Vein D	9.3	0.7	9.3	7.3	11.4	8.9	9.7
Artery A	6.3	0.8	6.3	4.6	8.6	5.7	6.8
Artery B	6.2	0.8	6.2	3.7	7.8	5.7	7.0
Artery C	6.1	1.0	6.1	2.9	10.2	5.5	6.6
Artery D	5.8	1.1	5.8	2.4	8.6	5.1	6.5
1st Angle	73.3	17.1	73.6	42.1	102.9	60.0	87.9
2nd Angle	77.1	19.0	76.9	9.5	125.0	65.4	87.6
3rd Angle	83.9	15.2	85.4	44.1	126.7	75.4	92.7

Table 2 – Evaluation of R&r in each SMA (%)

Arteries	A	B	C	D
CV R	2.8	5.0	2.5	2.6
CV r	7.7	5.6	8.9	11.1

Veins	A	B	C	D
CV R	0.4	0	0	0
CV r	4.7	3.8	4.2	3.6

Angles	1stGen	2ndGen	3rdGen
CV R	1.3	3.6	9.3
CV r	9.9	14.1	13.6

FIGURES

Fig. 1. First (yellow square), second (green square) and third (blue square) arteriolar bifurcations (a) defined as the junction between two daughter vessels (d1 and d2) and a mother vessel (M) (b). Fig. 1.b is a magnified image belonging to Fig. 1.a.

Fig. 2. Definition of standard measurement areas (SMA) identified with letters and identification of measurement guidelines (yellow lines) (a). Selection of the vessel measuring point for each SMA (arteries red dots, veins light blue dots) (b). Identification of the first, second and third arteriolar bifurcations (red dots) (c).

Fig. 3. Semi-automatic measurement of the vascular diameters (a) and arteriolar bifurcations (d). Manual selection of the vessel margins (b) and of the arteriolar branch (e) before automatic calculation of vascular diameter (c) and the inner angle α (f).

Fig. 4. Repeatability and reproducibility summary plot in arterial (a), venous vessels (b) and arteriolar bifurcations (c). The points traced in the graphs represent the deviations of the respective measurements from the average measurement for each individual part. Each operator is represented by a square. The height of the square represents an indication of the variability in measurements between tests. The length of the vertical lines containing the points joins together the various tests carried out by the same operator for each part.

Fig. 5. Tukey box plots of the comparison of measurements of healthy and hypertensive cats. All these comparisons are statistically significant at level P<0.001

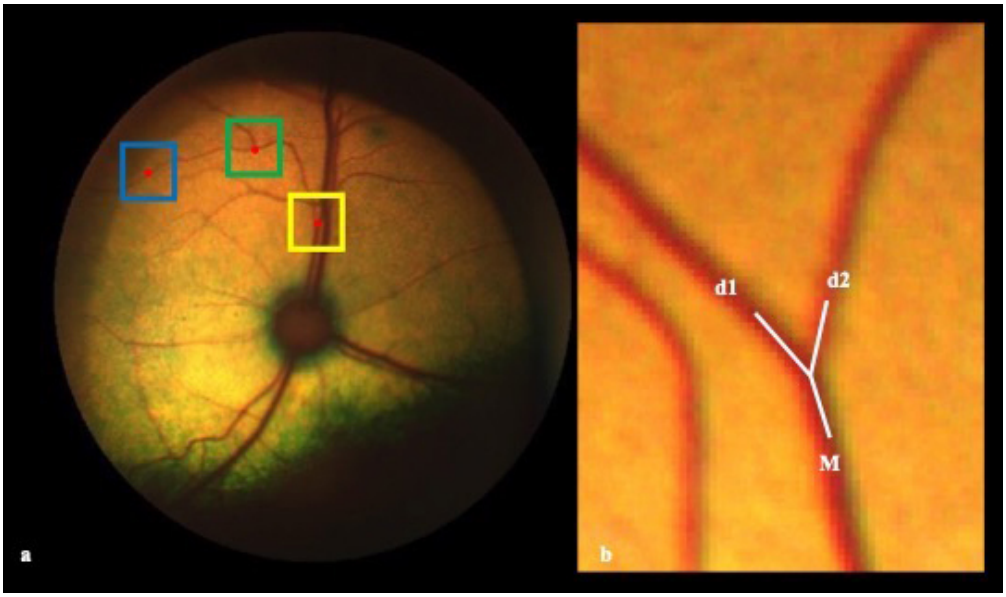

Fig. 1. First (yellow square), second (green square) and third (blue square) arteriolar bifurcations (a) defined as the junction between two daughter vessels (d1 and d2) and a mother vessel (M) (b). Fig. 1.b is a magnified image belonging to Fig. 1.a.

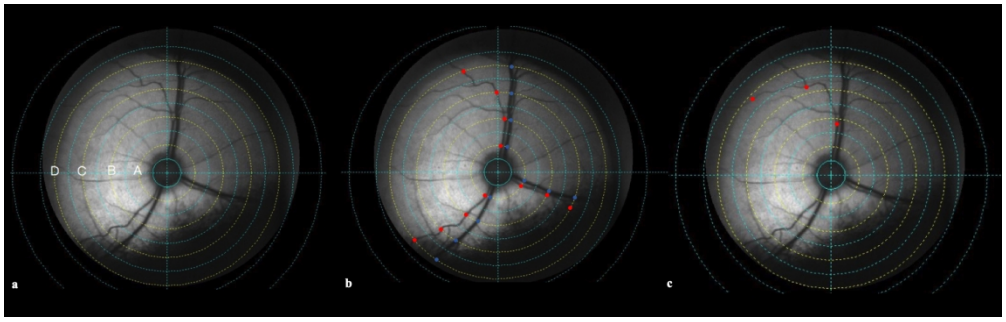

Fig. 2. Definition of standard measurement areas (SMA) identified with letters and identification of measurement guidelines (yellow lines) (a). Selection of the vessel measuring point for each SMA (arteries red dots, veins light blue dots) (b). Identification of the first, second and third arteriolar bifurcations (red dots) (c).

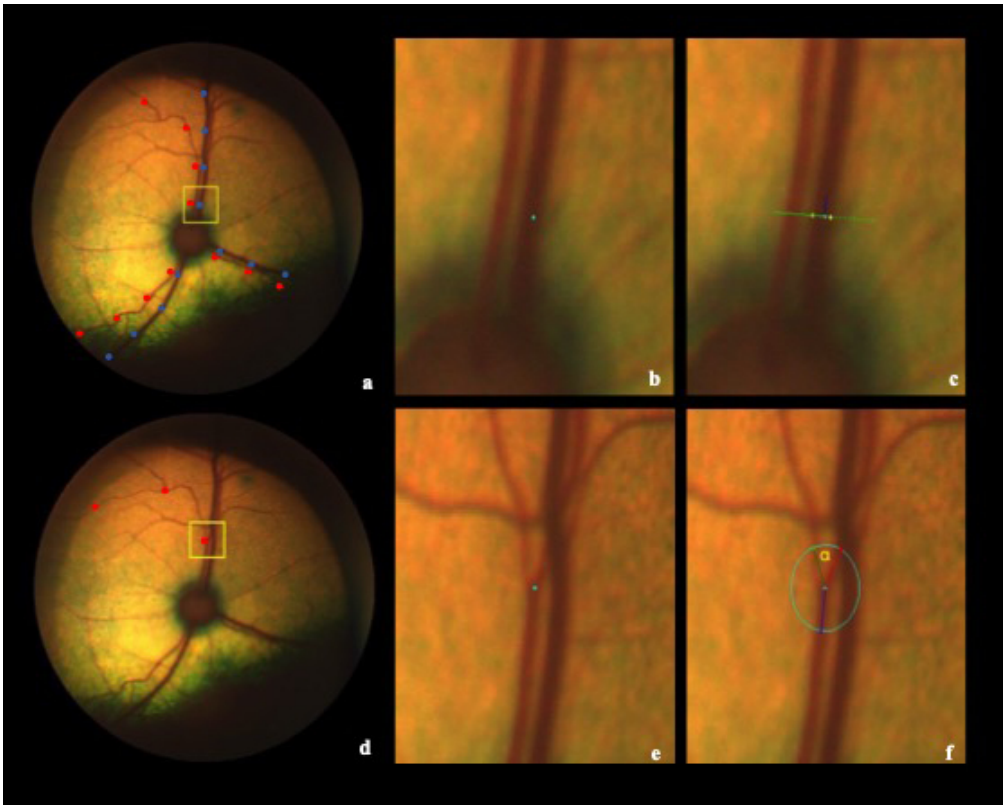

Fig. 3. Semi-automatic measurement of the vascular diameters (a) and arteriolar bifurcations (d). Manual selection of the vessel margins (b) and of the arteriolar branch (e) before automatic calculation of vascular diameter (c) and the inner angle α (f).

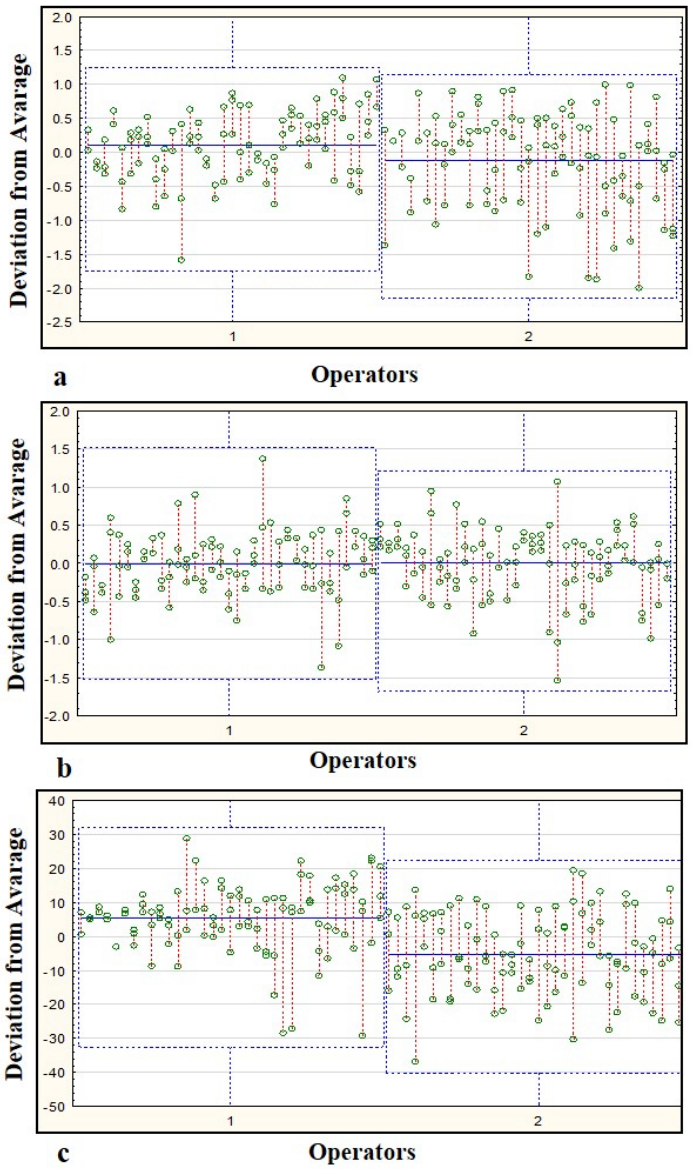

Fig. 4. Repeatability and reproducibility summary plot in arterial (a), venous vessels (b) and arteriolar bifurcations (c). The points traced in the graphs represent the deviations of the respective measurements from the average measurement for each individual part. Each operator is represented by a square. The height of the square represents an indication of the variability in measurements between tests. The length of the vertical lines containing the points joins together the various tests carried out by the same operator for each part.

51x86mm (300 x 300 DPI)

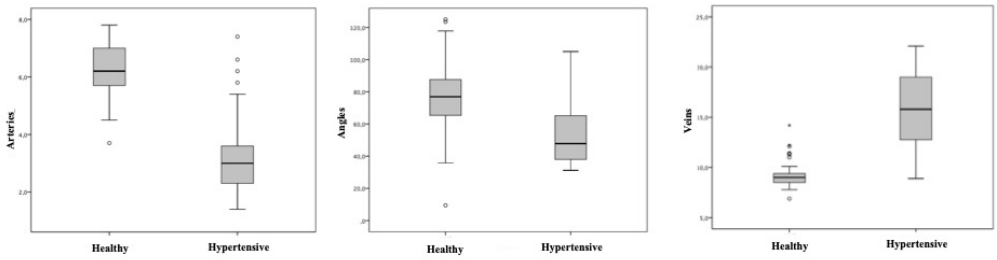

Fig. 5. Tukey box plots of the comparison of measurements of healthy and hypertensive cats. All these comparisons are statistically significant at level P<0.001

78x20mm (300 x 300 DPI)